Available online at www.sciencedirect.com
ScienceDirect
Bioorganic & Medicinal Chemistry 16 (2008) 5899–5907
Bioorganic & Medicinal Chemistry

Detection of triplet repeat sequences in the double-stranded DNA using pyrene-functionalized pyrrole–imidazole polyamides with rigid linkers

Jun Fujimoto, Toshikazu Bando,* Masafumi Minoshima, Shinsuke Uchida, Makoto Iwasaki, Ken-ichi Shinohara and Hiroshi Sugiyama*

Department of Chemistry, Graduate School of Science, Kyoto University, Kitashirakawa-Oiwakecho, Sakyo, Kyoto 606-8502, Japan

Received 15 March 2008; revised 23 April 2008; accepted 24 April 2008
Available online 27 April 2008

Abstract—Methods for sequence-specific detection in double-stranded DNA (dsDNA) are becoming increasingly useful and important as diagnostic and imaging tools. Recently, we designed and synthesized pyrrole (Py)–imidazole (Im) polyamides possessing two pyrene moieties, **1**, which showed an increased excimer emission in the presence of $(CAG)_{12}$-containing oligodeoxynucleotides (ODN) 1 and 2. In this study, we synthesized bis-pyrenyl Py–Im polyamides with rigid linkers **2**, **3**, and **4** to improve their fluorescence properties. Among the conjugates, **2** showed a marked increase in excimer emission, which was dependent on the concentration of the target ODN and the number of CAG repeats in the dsDNA. Unlike conjugate **1**, which has flexible linkers, the excimer emission intensity of **2** was retained at over 85%, even after 4 h. Py–Im polyamides have the potential to be important diagnostic molecules for detecting genetic differences between individuals.

1. Introduction

There is an ever-increasing clinical need to diagnose hereditary diseases in their early stages. Therefore, diagnostic molecules that directly detect specific double-stranded DNA (dsDNA) sequences without the need for denaturation, hybridization, washing, or labeling of the DNA samples are attractive research subjects.[1,2]

Minor groove-binding *N*-methylpyrrole (Py) and *N*-methylimidazole (Im) polyamides uniquely recognize each of the four Watson–Crick base pairs. An antiparallel pairing of imidazole opposite to pyrrole (Im/Py) recognizes a G–C base pair, whereas a Py/Py pair recognizes A–T or T–A base pairs. A β-alanine/β-alanine (β/β) pair reads T–A and A–T pairs in the same way as a Py/Py pair does.[3,4] Thus, Py–Im polyamides can sequence-specifically recruit various functional groups into DNA.[5,6] We have developed various types of sequence-specific alkylating Py–Im polyamides and have investigated their chemical and biological properties.[7–9] Recently, it has been shown that the sequence-specific binding properties of Py–Im polyamides are useful for the detection of specific sequences in duplex DNA. For example, Dervan and co-workers have focused on Py–Im polyamide–fluorophore conjugates[10–12] and novel fluorescent scaffolds of Py–Im polyamides without dye molecules.[13]

It is known that the continuous intergenerational expansion of simple trinucleotide CAG repeats in genomic DNA results in hereditary disorders, such as Huntington's disease, spinobulbar muscular atrophy, and several ataxias.[14] Therefore, small molecular probes that can detect the number of CAG repeat sequences have the potential to be important diagnostic tools for such hereditary neurological diseases.[15] We have already demonstrated that Py–Im polyamide **1** (Fig. 1), containing two pyrene moieties, shows a strong excimer fluorescence that depends on the number of CAG repeat sequences in dsDNA samples.[16] However, from the viewpoint of future biological applications, a longer excitation wavelength of pyrene-functionalized polyamides is desired. More importantly, the intensity of the

Keywords: DNA binder; Pyrrole–imidazole polyamide; Fluorescence detection; CAG repeat.
* Corresponding authors. Tel.: +81 75 753 4002; fax: +81 75 753 3670; e-mail addresses: bando@kuchem.kyoto-u.ac.jp; hs@kuchem.kyoto-u.ac.jp

0968-0896/$ - see front matter © 2008 Elsevier Ltd. All rights reserved.
doi:10.1016/j.bmc.2008.04.060

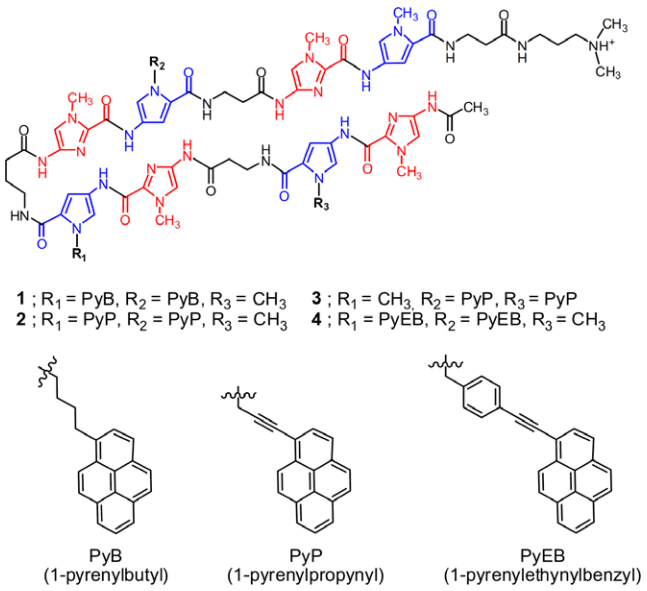

Figure 1. The chemical structures of bis-pyrenyl Py–Im polyamides with flexible butyl linkers **1**, and rigid linkers **2**, **3**, and **4**.

excimer emission of conjugate **1** is unsustainable, and decreases markedly within a period of several minutes after the addition of oligodeoxynucleotides (ODN) 1 and 2.

Taking these points into consideration, we newly synthesized and evaluated Py–Im polyamides with two pyrenes: **2**, **3**, and **4** (Fig. 1). The two pyrenes are attached to an internal pyrrole ring by rigid linkers in these molecular probes. Importantly, the excitation wavelengths of these conjugates are shifted to the red compared with conjugate **1**. In particular, conjugate **2** shows a stronger excimer signal than conjugate **1** does. Moreover, the excimer emission intensity of **2** is retained at over 85%, even after a period of 4 h.

2. Results and discussion

2.1. Molecular design

We have already reported Py–Im polyamide **1**, which recognizes a seven base pair sequence, 5′-AGCAGCA-3′, and shows excimer fluorescence.[16] Conjugate **1** was designed based on the concept of the molecular beacon.[17–23] As shown in Figure 2, we hypothesized a molecular interaction model. When polyamide binds to the target dsDNA, two pyrene moieties are located in close proximity, and excimer formation occurs exhibiting a consequent longer wavelength excimer emission. To improve the emission properties, we chose both a propynyl linker (for conjugates **2** and **3**) and an ethynylbenzyl linker (for conjugate **4**) as the rigid linker (Fig. 1). Recently, several researchers have shown the improved photochemical properties of various alkynylpyrenes or alkynylperylenes.[24–27] In addition, we expected that rigid linkers would restrict the geometry of the dye molecules, which could lead the two pyrene molecules to efficiently form an intramolecular excimer near the minor groove.

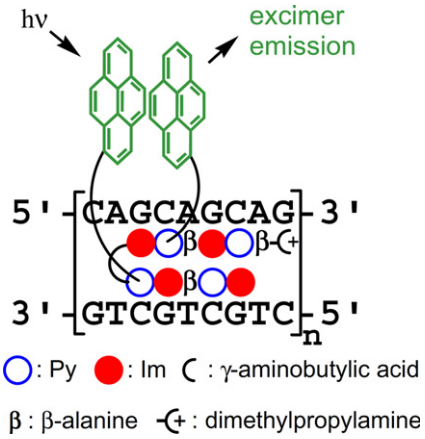

Figure 2. Schematic presentation of pyrene-functionalized Py–Im polyamide interactions with target dsDNA.

2.2. Monomer synthesis

We prepared 4-(9-fluorenylmethoxycarbonyl)amino-1-(2-propynyl)pyrrole-2-carboxylic acid (**8a**) and 4-(9-fluorenylmethoxycarbonyl)amino-1-(4-iodobenzyl)pyrrole-2-carboxylic acid (**8b**) according to the procedure shown in Scheme 1. Methyl 4-(*tert*-butoxycarbonyl)aminopyrrole-2-carboxylate (**6**) was synthesized from the starting material **5**[28,29] by subsequent reduction and protection using palladium–carbon and $(Boc)_2O$ under hydrogen gas. Although an amino pyrrole intermediate was formed under these conditions, the addition of $(Boc)_2O$ and TEA during the course of the reaction reduced any unreacted amine and provided **5** in a high yield. By using TEA in this reaction, the production of N1-Boc protected pyrrole was reduced to trace amount. Alkylation of the resultant **6** with propargyl bromide or 4-iodobenzyl bromide followed by hydrolysis using LiOH pro-

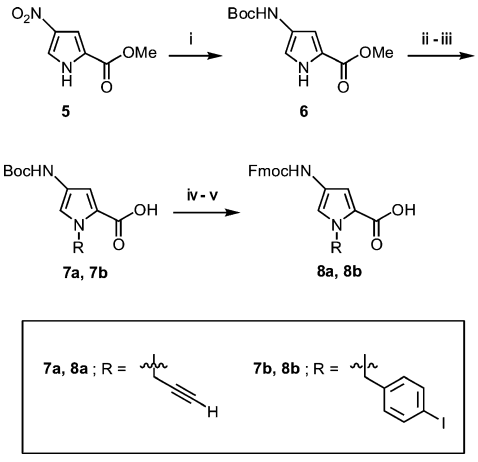

Scheme 1. Preparation of two new monomers for Fmoc solid-phase synthesis. Reagents: (i) H_2, Pd/C, $(Boc)_2O$, TEA, and DMF; (ii) propargyl bromide or 4-iodobenzyl bromide, K_2CO_3, tetra-*n*-butylammonium iodide, and acetone; (iii) LiOH, H_2O, and THF; (iv) 3 M HCl and AcOEt, (v) FmocONSu, $NaHCO_3$, H_2O, and DMF.

vided **7a** and **7b**. The removal of the *t*-Boc protecting group and subsequent Fmoc protection produced **8a** and **8b**, respectively.

2.3. Synthesis of conjugates 2–4

The synthetic schemes for conjugates **2**, **3**, and **4** are shown in Scheme 2. The polyamides were synthesized using an Fmoc solid-phase chemical synthesis method similar to a published procedure[30,31] using HCTU as the coupling reagent. After the completion of solid-phase synthesis, the polyamides were cleaved from the resins by aminolysis with *N*,*N*-dimethyl-1,3-propanediamine to produce polyamides **9**–**11**. Crude **9** was coupled with 1-bromopyrene using the Sonogashira method to produce the desired polyamide **2** possessing two pyrene moieties. From polyamide **10**, conjugate **3** was prepared using a synthetic procedure similar to that of **2**, and conjugate **4** was synthesized from the Sonogashira coupling of polyamide **11** with 1-ethynylpyrene. The structures of conjugates **2**–**4** were confirmed by electrospray ionization time-of-flight mass spectrometry (ESI-TOF-MS) after purification using reverse-phase HPLC. Purified polyamides were used for evaluation of their steady-state emission properties.

2.4. UV–visible absorption spectra, fluorescence spectra, and photophysical data

Figure 3 shows the UV–visible absorption and fluorescence spectra of bis-pyrenyl polyamides **1**–**4** in a DMF solution, and Table 1 lists the photophysical data for **1**–**4** (the absorption maxima, absorption coefficients, and the monomer emission maxima). Compared with conjugate **1**, conjugates **2** and **3** revealed a bathochromic shift of 20 nm in the absorption maximum derived from pyrene moieties, and the absorption peak of conjugate **4** was shifted 24 nm further into the red (Fig. 3 and Table 1). Similarly, the monomeric fluorescence maxima of conjugates **2**–**4** shifted to longer wavelengths as well (Fig. 3 and Table 1). These changes in absorption and fluorescence maxima indicate that the electronic properties of the bis-pyrenyl polyamides were improved by the extension of π-orbital conjugation via alkynyl bridges. Conversely, the absorption coefficients of the conjugates decreased consecutively with π-orbital extension.

2.5. Fluorescence of conjugates 2–4 in the presence of CAG repeat sequences

The fluorescence properties of the polyamides with two pyrene cores **2**, **3**, and **4** in the presence and absence of

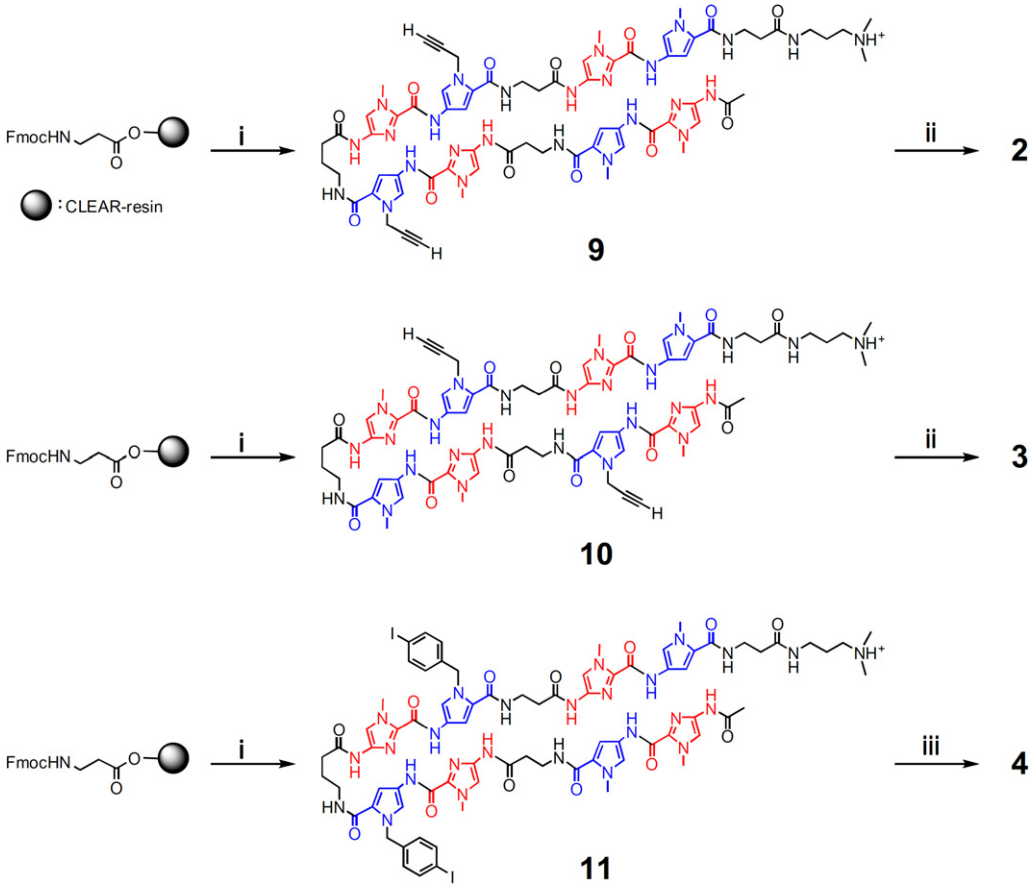

Scheme 2. Synthetic schemes for the preparation of bis-pyrenyl Py–Im polyamides **2**, **3**, and **4** with rigid linkers. Reagents: (i) Fmoc solid-phase synthesis was followed by processing with *N*,*N*-dimethyl-1,3-propanediamine; (ii) 1-bromopyrene, $[Pd(PPh_3)]_4$, CuI, TEA, and DMF; (iii) 1-ethynylpyrene, $[Pd(PPh_3)]_4$, CuI, TEA, and DMF.

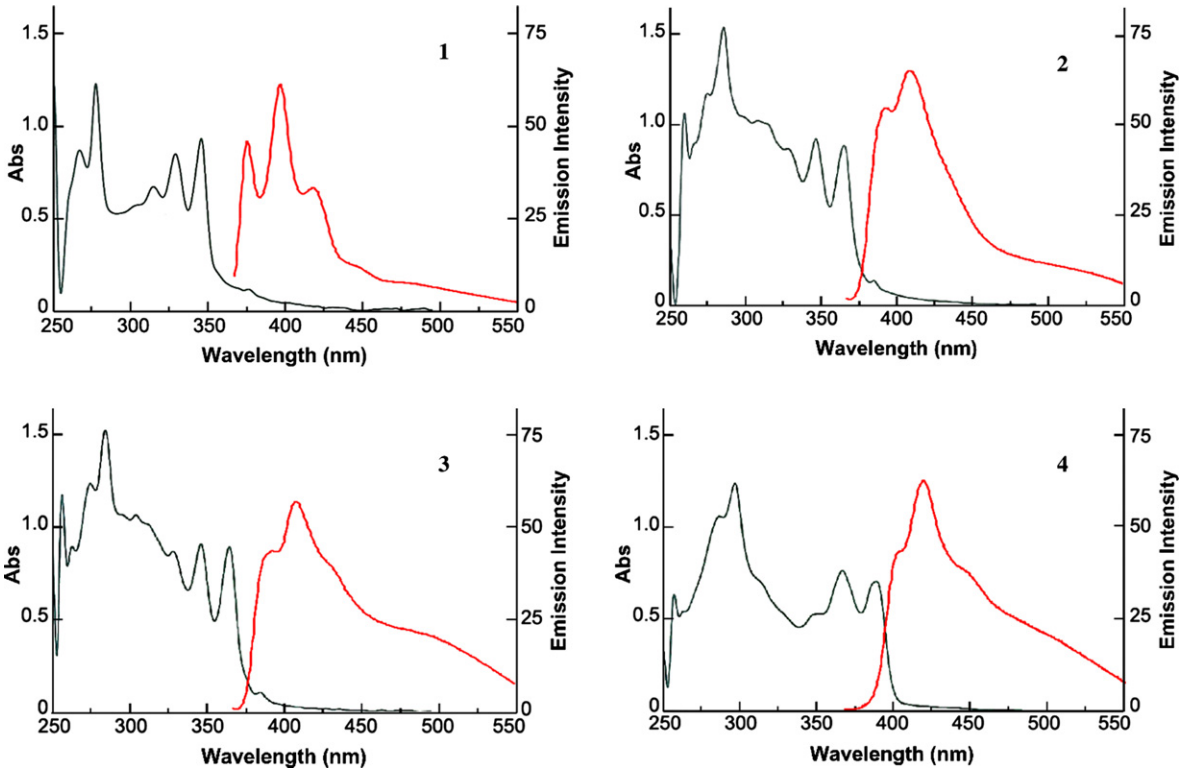

Figure 3. UV–visible absorption spectra (black) and fluorescence spectra (red) of **1**–**4** in DMF ([**1**] = [**2**] = [**3**] = [**4**] = 100 μM), λ_{em} = 345, 365, 365, and 363 nm for **1**–**4**.

Table 1. Photophysical data

Polyamide	λ_{abs}[a] (nm)	ε ($\times 10^4$) (mol^{-1} dm^3 cm^{-1})	λ_{em}[b] (nm)
1	345	9.4	398
2	365	9.1	409
3	365	9.1	409
4	389	7.1	417

[**1**] = [**2**] = [**3**] = [**4**] = 100 μM in DMF.
[a] λ_{abs} denotes the absorption maxima at the longest wavelength.
[b] λ_{em} denotes the fluorescence maxima at the longest wavelength.

the 41-mer $(CAG)_{12}$-containing ODN-1/2 (Fig. 4A) were examined. Initially, we confirmed that the excitation maxima of the hairpin polyamides with alkynylpyrenes **2**–**4** were longer than that of **1** (345 nm). Thus, the conjugates were irradiated at their excitation maxima (365 nm for conjugates **2** and **3**, and 363 nm for conjugate **4**), and the steady-state fluorescence spectra were measured. As a result, conjugate **2** showed a low background emission around 490 nm in the absence of the target duplex ODN-1/2, and a striking increase in emission centered at 495 nm with increasing concentration of ODN-1/2 (Fig. 4B). In contrast, the intensity of the corresponding bands for the pyrene monomer decreased, depending on the concentration of the target ODN-1/2. It is likely that the marked increase in long wavelength emission is derived from a pyrene excimer formed on binding of the polyamides to the minor groove of the dsDNA. Moreover, conjugate **2** revealed a bathochromic shift of 20 nm in the excimer emission maxima because of π-orbital extension via alkynyl linkers. While conjugate **3** also showed excimer fluorescence that depended on the concentration of ODN-1/2, the excimer emission of conjugate **3** was much weaker than that of **1** (Fig. 4C). The monomer emission of **3** is quenched, even in the absence of ODN, probably because the Py–Im polyamide scaffold interacts with the pyrene moieties in the sample solution. The difference in the spectra of **2** and **3** indicates that the point of attachment of the pyrene molecules in the polyamides has a critical influence on the fluorescence properties, as observed in our previous study.[16] In conjugate **4**, an excimer emission centered at 482 nm was observed without ODN-1/2, and the excimer intensity of **4** correlated weakly with the amount of target ODN (Fig. 4D). Conjugate **4** has hydrophobic phenyl groups as rigid linkers, which led the pyrene molecules to form an excimer, even in the absence of ODN. Of the conjugates that showed an enhanced excimer emission depending on the amount of the target DNA, we concluded that polyamide **2** was the most fascinating excimer-forming probe for the detection of CAG repeat sequences. Conjugate **2** showed optimal excimer fluorescence in the presence of target DNA sequences, while the pyrene excimer did not form in the absence of DNA. Furthermore, the excimer emission intensity of conjugate **2** at a DNA concentration of 5 μM was about two times higher than that of conjugate **1**, and approximately four times higher than that of conjugate **3**. We also noted that the ratio of the excimer intensity to the monomer intensity ($I_{excimer}/I_{monomer}$) in the presence of 5 μM target DNA had a value of 4.8 for conjugate **1** and 1.8 for conjugate **3**, while this increased to a value of 12.1 for conjugate **2**. These results suggest that the two pyrene molecules in conjugate **2** can form an excimer efficiently, which induces strong excimer emission.

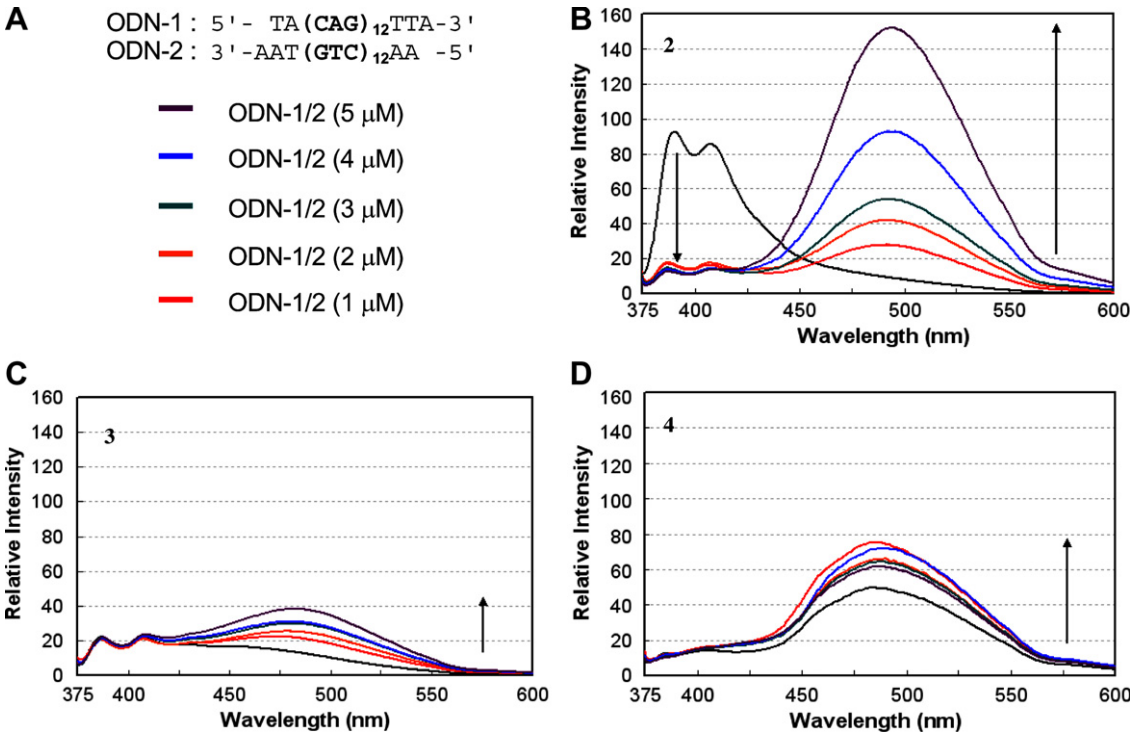

Figure 4. (A) Sequences of ODN-1 and ODN-2. (B) Fluorescence titration spectra of conjugate **2** (10 μM) in a 5 mM sodium phosphate buffer (pH 7, with 7% v/v DMF) in the presence of the target repeat sequence ODN-1/2 (0–5 μM). (C) Fluorescence titration spectra of conjugates **3** (10 μM) and (D) **4** (10 μM) in a 5 mM sodium phosphate buffer (pH 7, with 7% v/v DMF) in the presence of the target repeat sequence ODN-1/2 (0–5 μM), λ_{ex} = 365 nm for conjugates **2** and **3** or 363 nm for conjugate **4**.

2.6. Direct detection of the number of CAG repeat sequences in dsDNA using conjugate 2

Because it was found that conjugate **2** was a promising excimer-forming probe for dsDNA that contains CAG repeat sequences, we further investigated whether this excimer emission could be used to quantify the number of CAG repeat sequences. Four types of dsDNA consisting of different numbers of CAG repeats (Fig. 5A) were prepared, and the fluorescence properties of polyamide **2** in the presence of these sample DNAs were examined. A strong excimer emission of conjugate **2** was observed that depended on the number of CAG repeat sequences (4–12), as shown in Figure 5B ([DNA] = 5 μM). Conversely, the excimer emission was extremely weak using ODN-7/8 or −9/10, without CAG repeats. This weak background signal would result in a higher signal-to-noise ratio (S/N). Unexpectedly, the monomer emission quenched in the presence of the mismatched ODN-7/8 or −9/10. In addition, it is worth noting that conjugate **2** could also distinguish the number of CAG repeats at DNA concentrations of 1–4 μM as well (Fig. 5C). These results indicate the possible application of conjugate **2** to the quantification of CAG repeat sequences in duplex DNA.

2.7. Thermal stability of the excimer formation of conjugate 2

conjugate **1** as a biological tool to detect CAG triplet repeat sequences, there is a serious problem in that the excimer intensity of **1** decreases markedly with time. Therefore, we examined the change in excimer fluorescence of conjugate **2** with time. Figure 6 shows that the excimer intensity of conjugate **2**, with propynyl linkers (blue), was retained at over 85%, even after 4 h, while that of **1**, with butyl linkers (red), decreased to less than half within a period of 30 min. Although the reason why the excimer intensity of conjugate **2** is maintained is unclear, as far as we are aware, this is the first report demonstrating that a decrease in the excimer emission intensity may be prevented via the introduction of a rigid linker.

2.8. Surface plasmon resonance assay

To obtain further insight into the interactions of conjugate **2** with target sequences, the binding affinity of polyamide **2** and the parent Py–Im polyamide was investigated using surface plasmon resonance (SPR) methods and biotinylated hairpin DNA. The dissociation equilibrium constant (K_D) was obtained by fitting the resulting sensorgrams (Fig. 7A and B) to a theoretical model. The value of K_D for **2** was determined to be 8.37×10^{-7} M, which represents approximately a 60 times lower binding affinity of **2** than that of the parent ($K_D = 1.39 \times 10^{-8}$ M). A similar retardation of binding has also been observed by Dervan and co-workers, where they observed using quantitative footprinting titration that the binding affinity of polyamides with TMR at DNA match sites was reduced by a factor of 10–50 from the parent polyamides (R = CH_3).[10] Although the introduction of bulky pyrenyl groups weakens binding to the DNA minor groove, the rigid

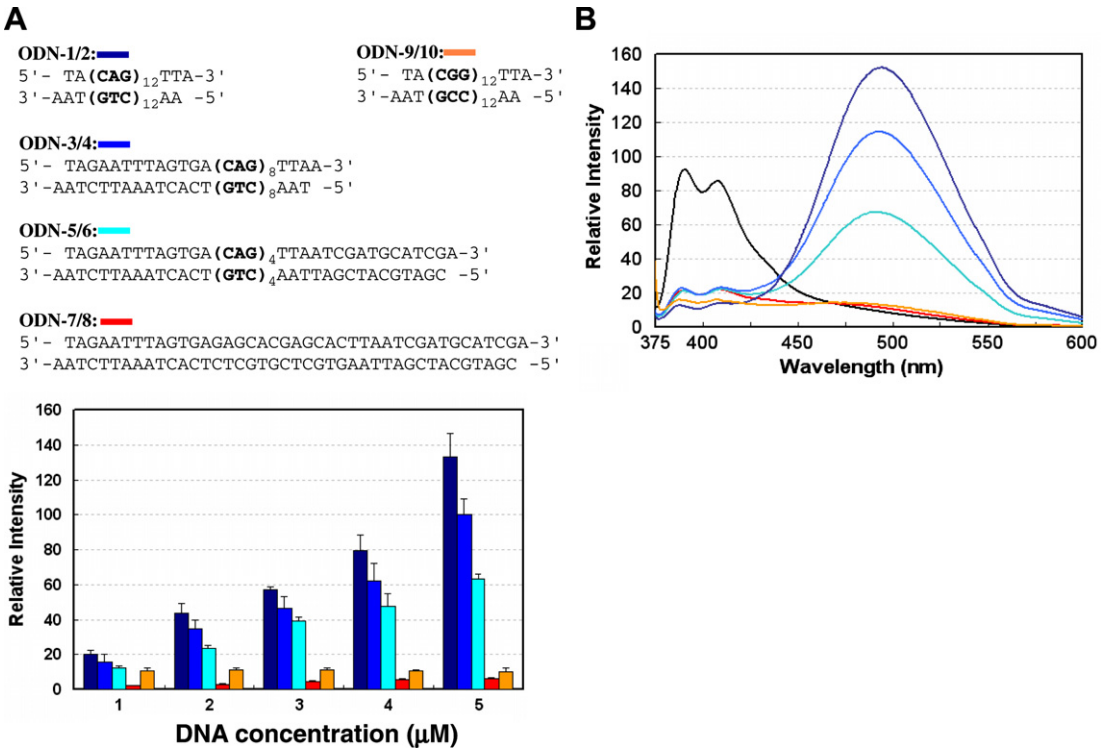

Figure 5. (A) Sequences of ODN 1–10. (B) Fluorescence titration spectra of conjugate **2** (10 μM) in a 5 mM sodium phosphate buffer (pH 7, with 7% v/v DMF) in the presence of each ODN (5 μM). The black line shows the spectrum in the absence of ODN. (C) Fluorescence titration graph of conjugate **2** ([**2**] = 10 μM, [sodium phosphate] = 5 mM, 7% v/v DMF, at pH 7, λ_{em} = 495 nm) in the presence of each ODN (1–5 μM). The relative intensity was obtained by subtracting the background level of emission of **2** in the absence of ODN at 495 nm. The error bars denote the standard deviation of the mean of triplicate samples, λ_{ex} = 365 nm.

propynyl linker of conjugate **2** adjusts the binding location, allowing the formation of excimer fluorescence.

3. Conclusions

We have successfully synthesized bis-pyrenyl Py–Im polyamides with rigid linkers **2**, **3**, and **4** using Fmoc solid-phase synthesis and a subsequent Sonogashira coupling reaction. The steady-state fluorescence spectra of the conjugates were measured to evaluate their fluorescence properties. Among the conjugates studied, pyrene-functionalized conjugate **2**, with propynyl linkers, showed a clear increase in excimer emission that depended on the concentration of the target ODN and the number of CAG repeats in the target dsDNA. Importantly, the excimer emission intensity of conjugate **2** was retained at over 85% even after 4 h. These findings pave the way for the development of diagnostic tools for detecting genetic differences between individuals.

4. Experimental

4.1. Materials

Reagents and solvents were purchased from standard suppliers and used without further purification. Abbreviations of some reagents: HCTU, 1-[bis(dimethylamino)methylene]-5-chloro-1*H*-benzotriazolium 3-oxide-hexafluorophosphate; $(Boc)_2O$, di-*tert*-butyl dicarbonate; TEA, triethylamine; FmocONSu, 9-fluorenylmethyl succinimidyl carbonate; DMF, *N*,*N*-dimethylformamide; DCM, dichloromethane; AcOEt, ethyl acetate; Et_2O, diethylether; THF, tetrahydrofuran. NMR spectra were recorded with a JEOL JNM-FX 400 nuclear magnetic resonance spectrometer, and tetramethylsilane was used as the internal standard. Proton NMR spectra were recorded in parts per million (ppm) downfield relative to tetramethylsilane. The following abbreviations apply to spin multiplicity: s (singlet), d (doublet), t (triplet), m (multiplet), br (broad). Electrospray ionization mass spectrometry (ESI-MS) and electrospray ionization time-of-flight mass spectrometry (ESI-TOF-MS) were performed on API150 (PE SCIEX) and BioTOF II (Bruker Daltonics) mass spectrometers. DNA oligonucleotides were purchased from Sigma–Aldrich Co. Fluorescence measurements were performed on Spectrofluorometer FP-6300 (JASCO). All machine-assisted polyamide syntheses were performed on Liberty Microwave Peptide Synthesizer (CEM Co.) with a computer-assisted operation system at a 0.10 mmol scale (200 mg of CLEAR resin, 0.52 meq/g) by using Fmoc solid-phase chemistry. HPLC purification was performed with a Chemcobond 5-ODS-H reversed-phase column (10 × 150 mm) in 0.1% AcOH with acetonitrile as eluent at a flow rate of 6.0 mL/min, appropriate gradient elution conditions, and detection at 254 or 365 nm.

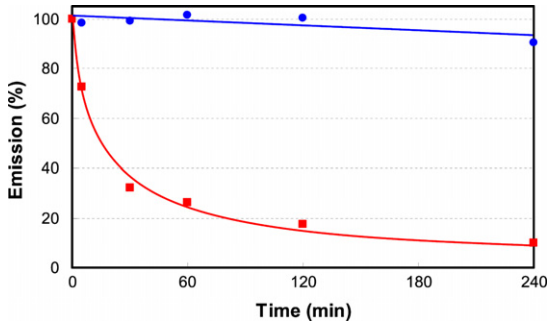

Figure 6. Time-course measurements of the fluorescence intensity of conjugates **1** (red) and **2** (blue) ([**2**] = 10 μM, [sodium phosphate] = 5 mM, 7% v/v DMF, at pH 7, λ_{em} = 475 nm for **1** and 495 nm for **2**) in the presence of ODN-1/2 (5 μM). The relative intensity was obtained by subtracting the background level of the emission of **1** and **2** in the absence of ODN at 475 nm (**1**) and 495 nm (**2**), λ_{ex} = 345 nm (**1**) and 365 nm (**2**).

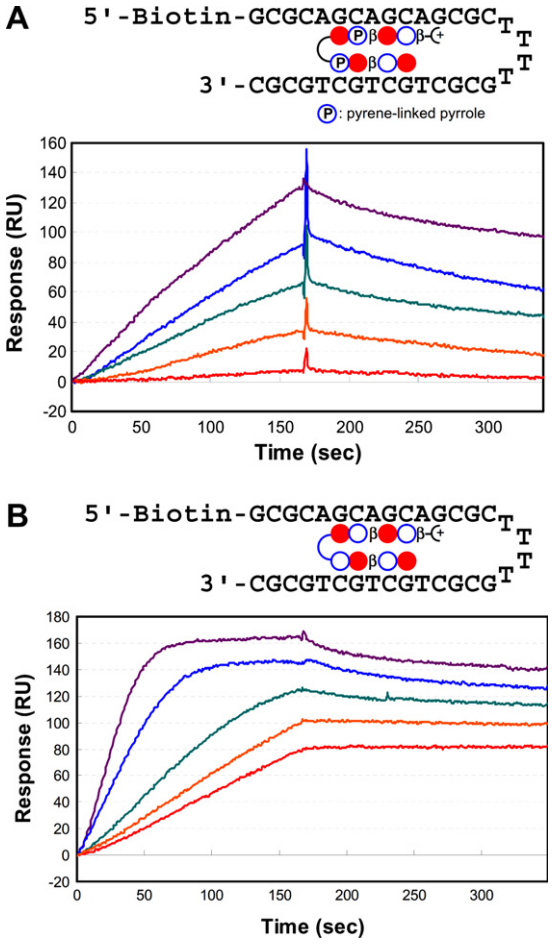

Figure 7. SPR sensorgrams for the interaction of: (A) conjugate **2**, and (B) parent Py–Im polyamide with hairpin DNAs immobilized on the surface of a sensor chip SA. All the experiments were performed in HBS-EP buffer (0.01 M HEPES, pH 7, 0.15 M NaCl, 3 mM EDTA, 0.005% surfactant P20) with 7.0% DMSO (v/v) at 25 °C, [**2**] = 625 nM (lowest curve)–10 μM (highest curve), [parent] = 112 nM (lowest curve)–894 nM (highest curve).

4.1.1. Methyl-4-(*tert*-butoxycarbonyl)aminopyrrole-2-carboxylate (6). To a solution of compound **5** (5.01 g, 29.5 mmol) in DMF (90 mL) was slowly added 10% Pd/C (280 mg). After TEA (6.20 mL, 44.2 mmol) and $(Boc)_2O$ (7.70 g, 35.3 mmol) were added dropwise, the reaction mixture was stirred for 17 h at room temperature under hydrogen gas pressure. Then, TEA (4.10 mL, 29.5 mmol) and $(Boc)_2O$ (6.80 g, 29.5 mmol) were added again, and the reaction mixture was stirred for another 3 h. The catalyst was removed by filtration through Celite using AcOEt/hexane (1:1, 500 mL). The organic phase was separated, washed with water (3× 200 mL), and saturated NaCl (200 mL), then dried over anhydrous Na_2SO_4. After filtration, the solvent was evaporated in vacuo to produce compound **6** (6.48 g, 92% yield) as a red powder. ^{1}H NMR (400 MHz, DMSO-d_6) δ = 11.54 (br s, 1H), 9.08 (s, 1H), 6.94 (s, 1H), 6.58 (s, 1H), 3.71 (s, 3H), 1.42 (s, 9H); ESI-TOF-MS: *m/z* calcd for $C_{11}H_{17}N_2O_4$: $[M+H]^+$ 241.12. Found: 241.18.

4.1.2. 4-(*tert* -Butoxycarbonyl)amino-1-(2-propynyl)pyrrole-2-carboxylic acid (7a). To a solution of compound **6** (2.41 g, 10.0 mmol) in toluene/H_2O (3:1, 40 mL) were added K_2CO_3 (4.15 g, 30.0 mmol) and Bu_4NI (0.74 g, 2.00 mmol). After propargyl bromide (5.57 mL, 50.0 mmol) was added, the reaction mixture was stirred for 14 h at 40 °C. After adding water (50 mL) and AcOEt (50 mL), the solution was partitioned between the organic solution and water. The organic phase was separated, washed with water (3× 50 mL), and saturated NaCl (50 mL), then dried over anhydrous Na_2SO_4. After filtration, the solution was concentrated to a brown residue, which was used in the next step without further purification. To a solution of crude product in water/MeOH (1:2, 30 mL) was added LiOH monohydrate (8.40 g, 200 mmol). The reaction mixture was stirred for 4 h at 50 °C, quenched by acetic acid (1.5 mL), and then AcOEt (200 mL) was added. The organic phase was separated, washed with water (3× 100 mL), saturated NaCl (100 mL), dried over anhydrous Na_2SO_4. After the filtration, the solution was concentrated to a residue, which was subjected to column chromatography (silica gel, 50% AcOEt in hexane) to produce compound **7a** (1.75 g, 66% yield for two steps) as a white powder. ^{1}H NMR (400 MHz, $CDCl_3$) δ = 8.08 (br s, 1H), 7.46 (s, 1H), 6.77 (s, 1H), 6.26 (s, 1H), 5.10 (d, J = 2.8 Hz, 2H), 2.40 (s, 1H), 1.48 (s, 9H); ESI-TOF-MS: *m/z* calcd for $C_{13}H_{17}N_2O_4$: $[M+H]^+$ 265.12. Found: 265.18.

4.1.3. 4-(*tert*-Butoxycarbonyl)amino-1-(4-iodobenzyl)pyrrole-2-carboxylic acid (7b). To a solution of compound **6** (2.20 g, 9.16 mmol) in acetone (80 mL) were added K_2CO_3 (3.80 g, 27.5 mmol) and Bu_4NI (0.68 g, 1.83 mmol). After 4-iodobenzyl bromide (3.00 g, 9.62 mmol) was added, the reaction mixture was stirred for 15 h at 50 °C. Evaporation of the solvent gave a brown residue, which was collected by filtration, washed with water, then dried to produce a yellow powder, which was used in the next step without further purification. To a solution of crude product in water/THF (1:2, 30 mL) was added LiOH monohydrate (7.69 g, 183 mmol). The reaction mixture was stirred for 2 days at 50 °C, quenched by acetic acid (1.8 mL), and then

AcOEt (200 mL) was added. The organic phase was separated, washed with water (3× 100 mL), and saturated NH_4Cl (100 mL), then dried over anhydrous Na_2SO_4. After filtration, the solution was evaporated in vacuo to produce compound **7b** as a red-brown powder. ^1H NMR (400 MHz, $CDCl_3$) δ = 7.41 (d, J = 3.9 Hz, 2H), 7.00 (br s, 1H), 6.79 (d, J = 3.9 Hz, 2H), 6.61 (s, 1H), 6.35 (br s, 1H), 5.29 (br s, 2H), 1.44 (s, 9H); ESI-TOF-MS: m/z calcd for $C_{17}H_{20}IN_2O_4$: $[M+H]^+$ 443.05. Found: 443.14.

4.1.4. 4-(9-Fluorenylmethoxycarbonyl)amino-1-(2-propynyl)pyrrole-2-carboxylic acid (8a). The reaction mixture of compound **7a** (2.50 g, 9.46 mmol) in 12 M HCl/AcOEt (1:3, 60 mL) was stirred for 4 h at room temperature. Evaporation of the solvent gave a brown residue, which was used in the next step without further purification. To a solution of crude product in water/DMF (2:3, 130 mL) was added $NaHCO_3$ (4.20 g, 50.0 mmol) and FmocONSu (3.51 g, 10.4 mmol). The reaction mixture was stirred for 14 h at room temperature under Argon gas. After the quenching by 5% aq HCl, the precipitate was collected by filtration, and then dried to produce **8a** (2.46 g, 67% yield for two steps) as a brown powder. ^1H NMR (400 MHz, $CDCl_3$) δ = 7.77 (d, J = 3.7 Hz, 2H), 7.60 (d, J = 3.7 Hz, 2H), 7.47 (s, 1H), 7.40 (t, J = 7.4 Hz, 2H), 7.31 (t, J = 7.4 Hz, 2H), 6.82 (s, 1H), 6.47 (s, 1H), 5.11 (s, 2H), 4.50 (d, J = 3.2 Hz, 2H), 4.25 (t, J = 6.4 Hz, 1H), 2.41 (s, 1H); ESI-TOF-MS: m/z calcd for $C_{23}H_{19}N_2O_4$: $[M+H]^+$ 387.13. Found: 387.27.

4.1.5. 4-(9-Fluorenylmethoxycarbonyl)amino-1-(4-iodobenzyl)pyrrole-2-carboxylic acid (8b). The reaction mixture of compound **7b** (3.98 g, 9.00 mmol) in 12 M HCl/AcOEt (1:3, 100 mL) was stirred for 8 h at room temperature. The precipitate was collected by filtration and dried to produce a brown powder (2.00 g). To a solution of crude product in water/DMF (1:3, 40 mL) were added $NaHCO_3$ (1.77 g, 21.1 mmol) and FmocONSu (1.78 g, 5.28 mmol). The reaction mixture was stirred for 18 h at room temperature under Argon gas. After the quenching by 5% aq HCl, DCM (300 mL) and water (300 mL) were added. The organic phase was separated, and washed with water (3× 300 mL), then saturated NH_4Cl (20 mL), dried over anhydrous Na_2SO_4. After the filtration, the solution was concentrated to a residue, which was subjected to column chromatography (silica gel, 25% AcOEt in hexane) to produce compound **8b** (1.92 g, 37% yield for four steps) as a brown powder. ^1H NMR (400 MHz, DMSO-d_6) δ = 12.20 (br s, 1H), 9.49 (s, 1H), 7.89 (d, J = 3.8 Hz, 2H), 7.70 (d, J = 3.8 Hz, 2H), 7.65 (d, J = 4.0 Hz, 2H), 7.41 (t, J = 7.4 Hz, 2H), 7.33 (t, J = 7.4 Hz, 2H), 7.18 (s, 1H), 6.85 (d, J = 4.0 Hz, 2H), 5.44 (s, 2H), 4.43 (d, J = 3.4 Hz, 2H), 4.26 (t, J = 6.4 Hz, 1H); ESI-TOF-MS: m/z calcd for $C_{27}H_{22}IN_2O_4$: $[M+H]^+$ 565.06. Found: 565.18.

4.1.6. AcImPy-β-ImPy^{propynyl} -γ-ImPy^{propynyl}-β-ImPy-β-Dp (9). Fmoc-β-Ala-CLEAR-acid resin (200 mg, 0.10 mmol) was swollen in 3 mL of DMF in a 50-mL plastic centrifuge tube for 30 min and placed on the board of a microwave synthesizer. DMF, DCM, 20% piperidine in DMF, 20% acetic anhydride in DMF, 0.45 M HCTU in DMF, 2 M ^{i}-Pr_2NEt in DMF were placed in the external bottles. Amino acids were weighed to give 4 molar excess amounts, and DMF was added to give standard 0.2 M amino acid solutions for use on the instrument. Each monomer in DMF solution was placed, respectively, in the loading position of the microwave synthesizer. The synthesis was then started, controlled by computer using the established program. The reactions were performed using deprotection steps of 180 s at 30 W (T_{max} = 75 °C) and coupling steps of 300 s at 25 W (T_{max} = 75 °C) and a final capping step of 120 s at 50 W (T_{max} = 75 °C). All couplings were carried out with single-couple cycles. After the completion of the synthesis on the peptide synthesizer, the resin was washed four times with DMF, methanol, and DCM, respectively, and dried in a desiccator at room temperature in vacuo. The resin (137 mg 57.0 μmol) was then placed in a 10-mL glass scintillation vial, 2 mL of *N*,*N*-(dimethylamino)propylamine was added, and the solution was stirred at 55 °C overnight. The resin was removed by filtration through a pad of Celite and washed thoroughly with DCM. The solvent of the filtrates was removed in vacuo, and the residue was used in the next step without further purification. ESI-TOF-MS: m/z calcd for $C_{68}H_{83}N_{26}O_{13}$: $[M+H]^+$ 1471.66. Found: 1471.90.

4.1.7. AcImPy^{propynyl} -β-ImPy-γ-ImPy^{propynyl}-β-ImPy-β-Dp (10). A synthetic procedure similar to that used for the preparation of compound **9** was followed to prepare compound **10**, using monomer **8a**. ESI-MS: m/z calcd for $C_{68}H_{83}N_{26}O_{13}$: $[M+H]^+$ 1471.66. Found: 1472.0.

4.1.8. AcImPy-β-ImPy^{iodoBn} -γ-ImPy^{iodoBn}-β-ImPy-β-Dp (11). A synthetic procedure similar to that used for the preparation of compound **9** was followed to prepare compound **11**, using monomer **8b**. ESI-MS: m/z calcd for $C_{76}H_{89}I_2N_{26}O_{13}$: $[M+H]^+$ 1827.52. Found: 1828.0.

4.1.9. AcImPy-β-ImPy^{PyB}-γ-ImPy^{PyB}-β-ImPy-β-Dp (1). Compound **1** was prepared by the reported procedure.[16]

4.1.10. AcImPy-β-ImPy^{PyP}-γ-ImPy^{PyP}-β-ImPy-β-Dp (2). To a solution of polyamide **9** in TEA/DMF (2:1, 1.8 mL), 1-bromopyrene (52.0 mg, 180 μmol), $Pd(PPh_3)_4$ (6.7 mg, 6.0 μmol), and CuI (1.1 mg, 6.0 μmol) were added. The reaction mixture was refluxed for 14 h under Argon gas. The solvent was removed in vacuo. The residue was washed with Et_2O and dissolved in approximately 0.5 mL of DMF. The polyamide solution was analyzed and purified by preparatory HPLC at 365 nm. Appropriate fractions were washed with Et_2O to give the final desired polyamide **2** (7.2 mg, 6.6% yield for 14 steps) as a yellow powder. ESI-TOF-MS: m/z calcd for $C_{100}H_{100}N_{26}O_{13}$: $[M+2H]^{2+}$ 936.61. Found: 936.66.

4.1.11. AcImPy^{PyP}-β-ImPy-γ-ImPy^{PyP}-β-ImPy-β-Dp (3). Compound **3** was prepared using a synthetic procedure similar to that used for the preparation of compound **2**, starting from Py–Im polyamide **10** (0.6 mg, 2.5% yield

for 14 steps). ESI-TOF-MS *m/e* calcd for $C_{100}H_{100}N_{26}O_{13}$: $[M+2H]^{2+}$ 936.61. Found: 936.47.

4.1.12. AcImPy-β-ImPy^{PyEB} -γ-ImPy^{PyEB}-β-ImPy-β-Dp (4). To a solution of polyamide **11** in TEA/DMF (2:1, 1.5 mL), 1-ethynylpyrene (24.9 mg, 110 μmol), $Pd(PPh_3)_4$ (5.6 mg, 5.0 μmol), and CuI (1.0 mg, 5.0 μmol) were added. The reaction mixture was stirred at 80 °C for 11 h under Argon gas. The solvent was removed in vacuo. The residue was washed with Et_2O and dissolved in about 0.5 mL of DMF. The polyamide solution was analyzed and purified by preparatory HPLC at 385 nm. Appropriate fractions were washed with Et_2O to give the final desired polyamide **4** (4.0 mg, 4.0% yield for 14 steps) as a yellow powder. ESI-TOF-MS: *m/z* calcd for $C_{112}H_{108}N_{26}O_{13}$: $[M+2H]^{2+}$ 1012.43. Found: 1012.53.

4.2. Steady-state fluorescence spectroscopy experiments

Steady-state fluorescence spectra were obtained using a FP-6300 Spectrofluorometer (JASCO) with an excitation wavelength of 365 nm (for conjugates **2** and **3**) or 363 nm (for conjugate **4**) in hybridization buffer, and oligonucleotides at corresponding concentrations of conjugates **2**–**4**. No special efforts were made to remove oxygen from the reaction solution at room temperature.

4.3. SPR assays

SPR experiments were performed on a Biacore *X* instrument at 25 °C. iotinylated hairpin DNA: 5′-biotin- labeled GGCCAGCAGCAGCGTATACGCTGCTGC TGGCC-3′ was obtained from Sigma–Aldrich Co. Streptavidin-functionalized SA sensor chips were purchased from Biacore. After immobilization of hairpin DNAs onto the sensor chips, measurements of binding curves of polyamides to the hairpin DNA, and data processing were performed according to following procedure: different concentrations of polyamide solutions in HBS-EP buffer with 7.0% DMSO were prepared by dilution from 10 mM stock solutions in DMSO. All binding experiments were carried out using HBS-EP buffer with 7.0% DMSO as running buffer, and the running buffer or 10 mM glycine–HCl (pH 1.5) was used as the regeneration solution. Typically, the buffer was injected at a flow rate of 5 μL/min as a blank control after a stable baseline was obtained, and then samples were injected under conditions identical to those of buffer injection at concentrations ranging from 625 nM to 10 μM for **2** and from 112 to 894 nM for parent Py–Im polyamide. Kinetic information was obtained by global fitting of the response units versus time using a model with mass transport effects using the BIA evaluation 4.1 program.

Acknowledgments

This work was supported by a Grant-in-Aid for Priority Research from the Ministry of Education, Culture, Sports, Science, and Technology, Japan. The authors acknowledge the support by the Global COE Program 'Integrated Materials Science' (#B-09).

References and notes

1. Ihara, T.; Mukae, M. *Anal. Sci.* **2007**, *23*, 625–629.
2. Ghosh, I.; Stains, C. I.; Ooi, A. K.; Segal, S. J. *Mol. Biosyst.* **2006**, *2*, 551–560.
3. Wemmer, D. E.; Dervan, P. B. *Curr. Opin. Struct. Biol.* **1997**, *7*, 355–361.
4. Dervan, P. B.; Edelson, B. S. *Curr. Opin. Struct. Biol.* **2003**, *13*, 284–299.
5. Dervan, P. B. *Bioorg. Med. Chem.* **2001**, *9*, 2215–2235.
6. Murty, M. S. R. C.; Sugiyama, H. *Biol. Pharm. Bull.* **2004**, *27*, 468–474.
7. Bando, T.; Sugiyama, H. *Acc. Chem. Res.* **2006**, *39*, 935–944.
8. Sasaki, S.; Bando, T.; Minoshima, M.; Shimizu, T.; Shinohara, K.; Takaoka, T.; Sugiyama, H. *J. Am. Chem. Soc* **2006**, *128*, 12162–12168.
9. Minoshima, M.; Bando, T.; Sasaki, S.; Shinohara, K.; Shimizu, T.; Fujimoto, J.; Sugiyama, H. *J. Am. Chem. Soc.* **2007**, *129*, 5384–5390.
10. Rucker, V. C.; Foister, S.; Melander, C.; Dervan, P. B. *J. Am. Chem. Soc.* **2003**, *125*, 1195–1202.
11. Rucker, V. C.; Dunn, A. R.; Sharma, S.; Dervan, P. B.; Gray, H. B. . H. B. *J. Phys. Chem. B* **2004**, *108*, 7490–7494.
12. Fechter, E. J.; Olenyuk, B.; Dervan, P. B. *J. Am. Chem. Soc* **2005**, *127*, 16685–16691.
13. Chenoweth, D. M.; Viger, A.; Dervan, P. B. *J. Am. Chem. Soc* **2007**, *129*, 2216–2217.
14. Mirkin, S. M. *Nature* **2007**, *447*, 932–940.
15. Nakatani, K.; Hagihara, S.; Goto, Y.; Kobori, A.; Hagihara, M.; Hayashi, G.; Kyo, M.; Nomura, M.; Mishima, M.; Kojima, C. *Nat. Chem. Biol.* **2005**, *1*, 39–43.
16. Bando, T.; Fujimoto, J.; Minoshima, M.; Shinohara, K.; Sasaki, S.; Kashiwazaki, G.; Mizumura, M.; Sugiyama, H. *Bioorg. Med. Chem.* **2007**, *15*, 6937–6942.
17. Yamanaka, K.; Iwai, T.; Ohtani, Y.; Sato, S.; Nakamura, M.; Nakano, H. *Bioconjug. Chem.* **2002**, *13*, 1266–1273.
18. Fujimoto, K.; Shimizu, H.; Inoue, M. . M. *J. Org. Chem.* **2004**, *69*, 3271–3275.
19. Okamoto, A.; Ichiba, T.; Saito, I. *J. Am. Chem. Soc.* **2004**, *126*, 8364–8365.
20. Yang, C. J.; Jockusch, S.; Vicens, M.; Turro, N. J.; Tan, W. *Proc. Natl. Acad. Sci. U.S.A.* **2005**, *102*, 17278–17283.
21. Seo, Y. J.; Hwang, G. T.; Kim, B. H. *Tetrahedron Lett.* **2006**, *47*, 4037–4039.
22. Oh, K. J.; Cash, K. J.; Plaxco, K. W. . K. W. *J. Am. Chem. Soc.* **2006**, *128*, 14018–14019.
23. Trkulja, I.; Biner, S. M.; Langenegger, S. M.; Häner, R. *ChemBioChem* **2007**, *8*, 25–27.
24. Yang, S. W.; Elangovan, A.; Hwang, K. C.; Ho, T. I. *J. Phys. Chem. B* **2005**, *109*, 16628–16635.
25. Gèci, I.; Filichev, V. V.; Pedersen, E. B. *Bioconjug. Chem.* **2006**, *17*, 950–957.
26. Maeda, H.; Maeda, T.; Mizuno, K.; Fujimoto, K.; Shimizu, H.; Inoue, M. *Chem. Eur. J.* **2006**, *12*, 824–831.
27. Astakhova, I. V.; Malakhov, A. D.; Stepanova, I. A.; Ustinov, A. V.; Bondarev, S. L.; Paramonov, A. S.; Korshun, V. A. *Bioconjug. Chem.* **2007**, *18*, 1972–1980.
28. Bremer, R. E.; Szewczyk, J. W.; Baird, E. E.; Dervan, P. B. *Bioorg. Med. Chem.* **2000**, *8*, 1947–1955.
29. Kumar, R.; Lown, J. W. *Org. Biomol. Chem.* **2003**, *1*, 3327–3342.
30. Wurtz, N. R.; Turner, J. M.; Baird, E. E.; Dervan, P. B. *Org. Lett.* **2001**, *3*, 1201–1203.
31. Belitsky, J. M.; Nguyen, D. H.; Wurtz, N. R.; Dervan, P. B. *Bioorg. Med. Chem.* **2002**, *10*, 2767–2774.